

Cite this: *J. Mater. Chem. A*, 2025, 13, 27726

Correction: Hybrid d^0 and d^{10} electronic configurations promote photocatalytic activity of high-entropy oxides for CO_2 conversion and water splitting

Jacqueline Hidalgo-Jiménez,^{ab} Taner Akbay,^c Xavier Sauvage,^d Lambert van Eijck,^e Motonori Watanabe,^{af} Jacques Huot,^g Tatsumi Ishihara^{af} and Kaveh Edalati^{*af}

DOI: 10.1039/d5ta90172c

rsc.li/materials-a

Correction for 'Hybrid d^0 and d^{10} electronic configurations promote photocatalytic activity of high-entropy oxides for CO_2 conversion and water splitting' by Jacqueline Hidalgo-Jiménez *et al.*, *J. Mater. Chem. A*, 2024, 12, 31589–31602, <https://doi.org/10.1039/D4TA04689G>.

The authors regret that in the original article, the scale bars in Fig. 4b and 5a were incorrect. The authors also regret errors in the orientation of the atomic planes in Fig. 6e. Additionally, the range of the X-axis in Fig. 9a was twice as large as the correct value, and two numbers in Table 3 were incorrectly shown as 12 and 2.95 instead of the correct values, 0.2 and 6.6. These unintentional errors do not affect any other data or the conclusions of the manuscript. The correct Fig. 4–6, 9 and Table 3 are as shown here.

^aInternational Institute for Carbon-Neutral Energy Research (WPI-I2CNER), Kyushu University, Fukuoka, Japan. E-mail: kaveh.edalati@kyudai.jp; Fax: +81 92 802 6744; Tel: +81 92 802 6744

^bDepartment of Automotive Science, Kyushu University, Fukuoka, Japan

^cMaterials Science and Nanotechnology Engineering, Yeditepe University, Istanbul, Turkey

^dUniv Rouen Normandie, INSA Rouen Normandie, CNRS, Groupe de Physique des Matériaux, UMR6634, 76000 Rouen, France

^eDepartment of Radiation Science and Technology, Delft University of Technology, Delft, Netherlands

^fMitsui Chemicals, Inc. – Carbon Neutral Research Center (MCI-CNRC), Kyushu University, Fukuoka, Japan

^gHydrogen Research Institute, Université du Québec à Trois-Rivières, Trois-Rivières, Canada



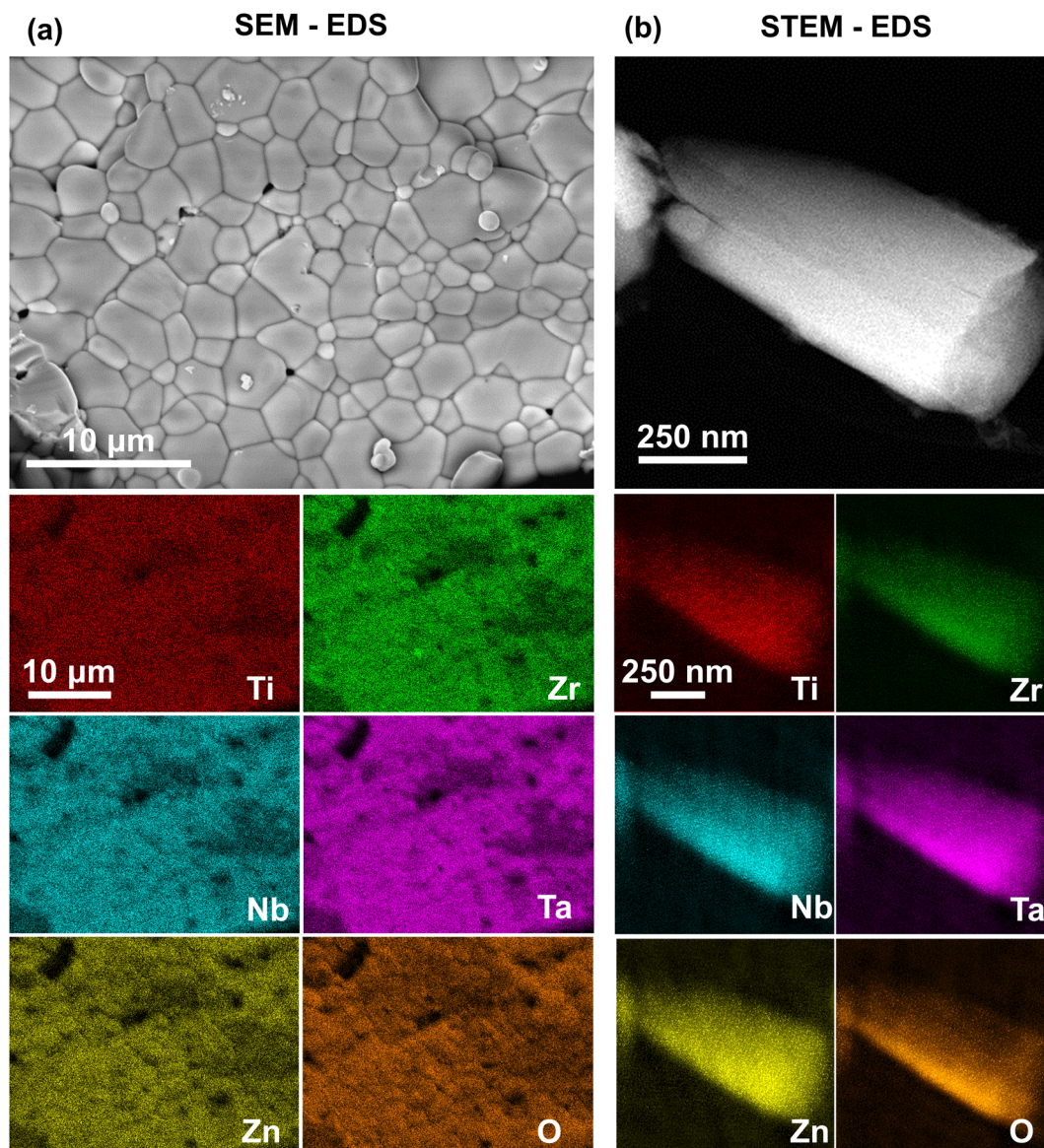


Fig. 4 Homogeneous distribution of elements at the micrometer and nanometer scales in high-entropy oxide TiZrNbTaZnO_{10} . (a) SEM-EDS and (b) STEM-EDS mappings.



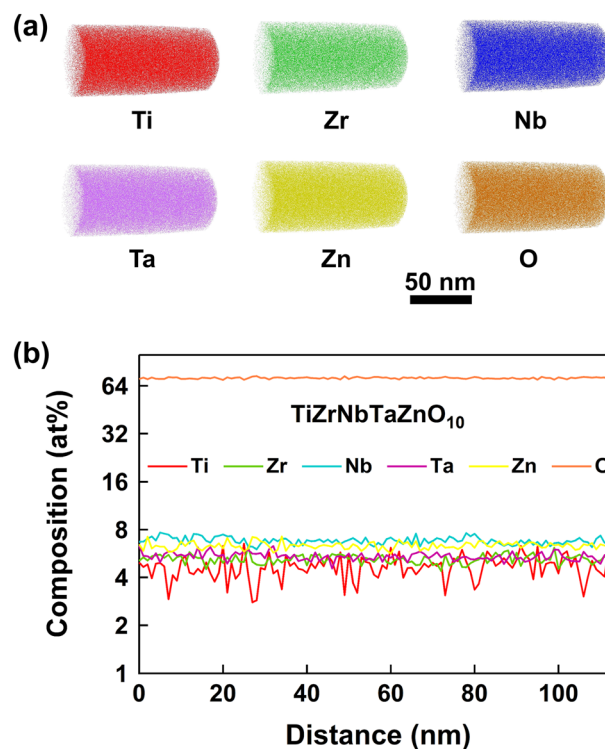


Fig. 5 Homogeneous distribution of elements at the atomic scale in high-entropy oxide TiZrNbTaZnO_{10} . (a) Three-dimensional chemical composition distribution and (b) percentage of elements along the sample tip.



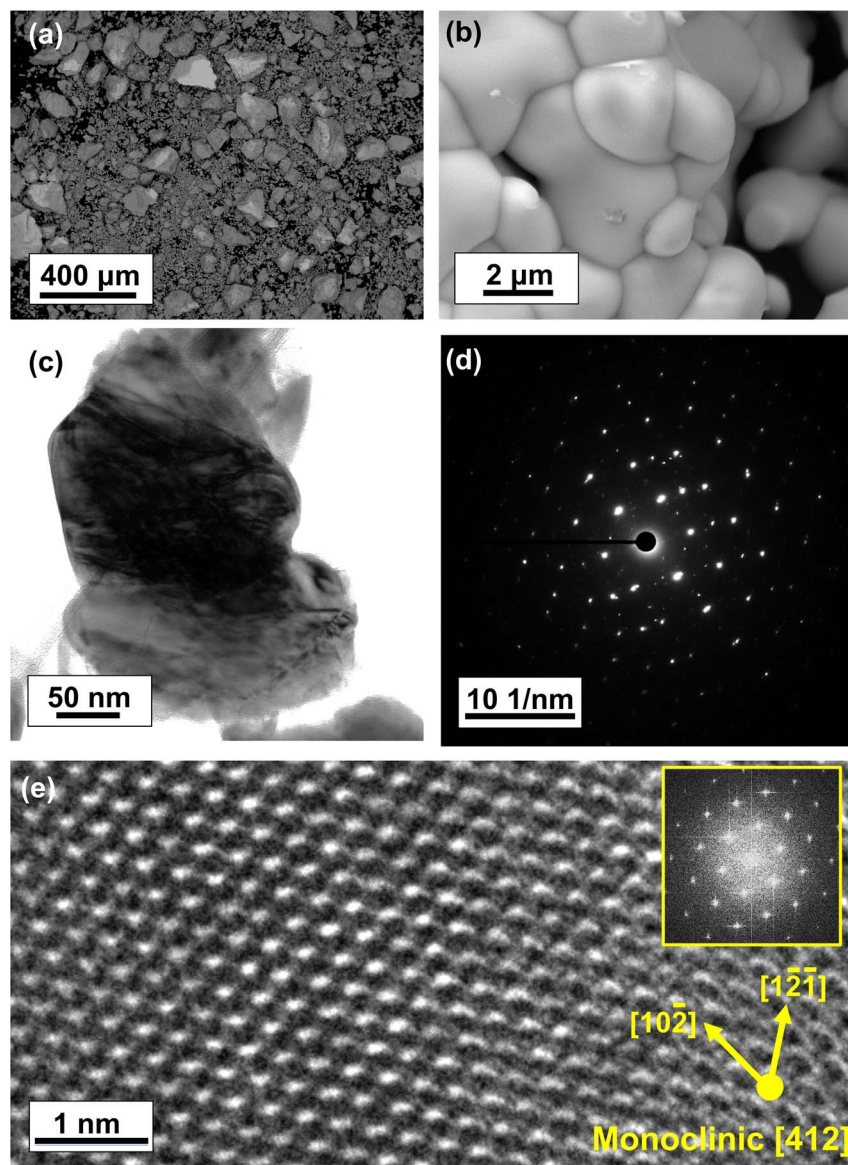


Fig. 6 Formation of micro-sized particles with a monoclinic structure in high-entropy oxide TiZrNbTaZnO_{10} . (a and b) SEM micrographs at different magnifications, (c) TEM bright-field micrograph, (d) SAED pattern, and (e) high-resolution image and corresponding fast Fourier transform.





Table 3 Catalyst mass, catalyst surface area, light source, rate of CO₂ conversion and amount of hydrogen production for several binary oxides, composites and high-entropy photocatalysts compared with TiZrNbTaZnO₁₀

Photocatalyst	Mass (mg)	Surface area (m ² g ⁻¹)	Light source	CO ₂ conversion (μmol hg ⁻¹)		CO ₂ conversion (μmol hm ⁻²)		Water splitting (mmol hg ⁻¹)		Water splitting (mmol hm ⁻²)		Ref.
				CO	CH ₄	CO	CH ₄	H ₂	H ₂	H ₂	H ₂	
TiO ₂ anatase	50	13.5	300 W Xe	—	—	—	—	0.3189	0.47	0.3189	0.47	39
TiO ₂ (HPT, ~70% columbite)	50	0.1	300 W Xe	—	—	—	—	0.005	1.08	0.005	1.08	39
TiO ₂ (HPT and anneal)	100 mg	6.8	300 W Hg	1.39	—	0.15	—	—	—	—	—	49
ZnO (HPT)	50	—	—	—	—	—	—	0.585	0.45	0.585	0.45	48
CeO _{2-x}	50	20.5	300 W Xe	1.68	—	0.081	—	—	—	—	—	50
Nb ₂ O ₅ /TiO ₂	100	57.3	200 W Xe	—	—	—	—	0.18	10.31	0.18	10.31	46
S doped Ta ₂ O ₅ -Cds	5	0.017	300 W Xe	—	—	—	—	0.2725	16.03	0.2725	16.03	51
MnCo/CN	—	—	300 W Xe	47	—	—	—	—	—	—	—	52
Cd _{1-x} Zn _x S	45	119	100 W LED	2.9	0.22	0.096	0.01	0.0361	0.2	0.0361	0.2	57
TiZrHfNbTaO ₁₁	100/50	0.089	400 W Hg/300 W Xe	4.6	—	5.16	—	0.027	134.76	0.027	134.76	4 and 10
TiZrHfNbTaO ₁₁	50	3	300 W Xe	—	—	—	—	—	—	—	—	54
(mechano-thermal synthesis)	—	—	—	—	—	—	—	—	—	—	—	—
TiZrHfNbTaO ₁₁ (laser crushing)	100	2.69	400 W Hg	50	200	1.66	6.66	0.0319	0.006	0.0319	0.006	24
TiZrHfNbTaO ₆ N ₃	100/50	2.3	400 W Hg, 300 W Xe	11.6	—	0.5	—	9.2	0.0002	9.2	0.0002	11 and 17
Ce _{0.2} Zr _{0.2} La _{0.2} Pr _{0.2} Y _{0.2} O ₂	2	61.4	11 W UV	—	—	—	—	0.415	—	0.415	—	12
ZrYCeCrO ₂ -based + 38 at% Ca	—	—	150 W Xe	—	—	—	—	6.61	0.29	6.61	0.29	13
Li(NbVtaCrMoWCo)O ₃	50	11.19	300 W Xe, 420 nm cutoff filter	—	—	—	—	—	—	—	—	15
(Co, Mn, Ni, Zn)O-metal organic framework	10	—	300 W Xe	—	—	—	—	13.24	—	13.24	—	16
Ce _{0.2} Zr _{0.2} La _{0.2} Pr _{0.2} Y _{0.2} O ₂	2	61.4	11 W UV	—	—	—	—	—	—	—	—	12
(Ca _{0.2} Cr _{0.2} Mn _{0.2} Ni _{0.2} Zn _{0.2}) ₃ O ₄	20	16.71	300 W Xe	23.01	2.89	0.03	0.65	—	—	—	—	8
Cu-(Ca _{0.2} Cr _{0.2} Mn _{0.2} Ni _{0.2} Zn _{0.2}) ₃ O ₄	20	42.08	300 W Xe	5.66	33.84	0.002	0.02	—	—	—	—	19
(NiCuMnCoZnFe) ₃ O ₄	30	66.48	—	15.89	8.03	0.007	0	—	—	—	—	20
TiZrNbTaZnO ₁₀	100/50	0.03	400 W Hg/300 W Xe	25.2	9.9	761.3	301	0.2	6.6	0.2	6.6	This study

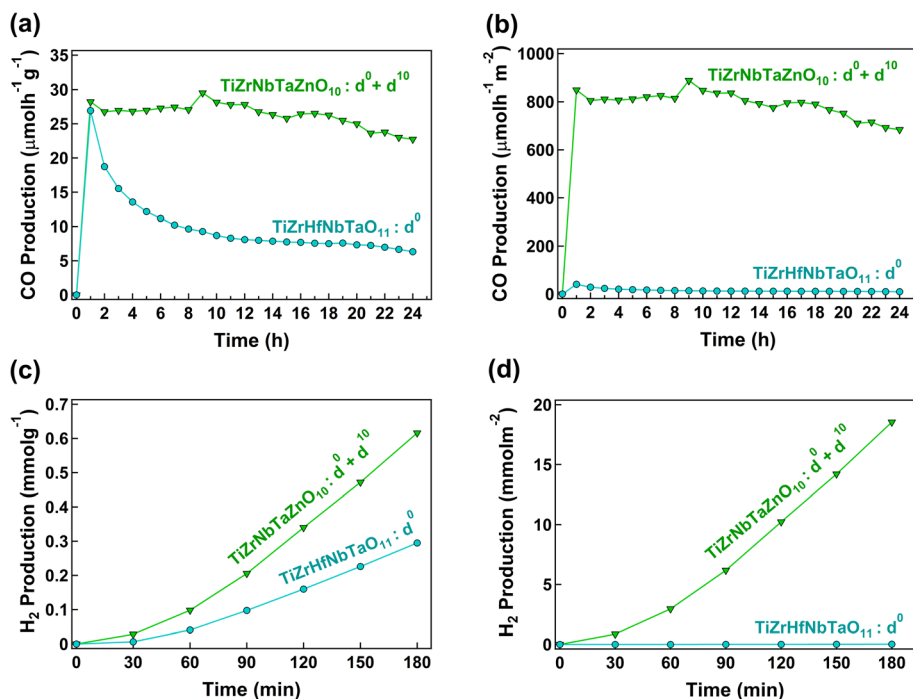


Fig. 9 Enhancement of the photocatalytic activity of high-entropy oxide TiZrNbTaZnO₁₀ compared to TiZrHfNbTaO₁₁ due to the mixed d⁰ and d¹⁰ electronic configuration. CO₂ to CO conversion rate per (a) unit mass and (b) surface area of the two catalysts. H₂ production from water splitting per (c) unit mass and (d) surface area of the two catalysts.

The Royal Society of Chemistry apologises for these errors and any consequent inconvenience to authors and readers.

